Spaces of Kleinian Groups
Lond. Math. Soc. Lec. Notes **xxx**, 1–36

Cambridge University Press, 2004
Y. Minsky, M. Sakuma & C. Series (Eds.)

Searching for the cusp

David J. Wright

Abstract

We discuss the process of algebraically finding cusps on the boundaries of deformation spaces of kleinian groups. The geometric starting point is an arrangement of circles with prescribed tangencies and relationships under a set of Möbius transformations. These lead to polynomial equations in several complex variables, which may then be numerically solved for the values which describe the cusp. We will go through this process for several deformation spaces corresponding to "plumbing" constructions of Maskit and Kra, and we will present some of the numerical output. The same techniques can also be used to calculate the coherent spiral hexagonal circle packings discovered by Peter Doyle, and we will compare the similarity factors of those packings to cusps on boundaries of deformation spaces.

1. Introduction

In this paper, we study the theoretical and numerical calculation of *maximal cusp groups* on the boundary of deformation spaces of kleinian groups. Specifically, we are interested in *maximally parabolic groups* which allow no deformations with a greater number of classes of parabolic elements.

The foundational study of cusp groups occurred in Bers' paper [Ber70] on boundaries of Teichmüller spaces. There he proved that the cusp groups form a set of measure zero in the boundary, and that there exist boundary groups he termed *totally degenerate*, for which the ordinary set is a single invariant domain. Then came a windstorm of ideas from Thurston, first in his celebrated *Geometry and Topology of 3-Manifolds* and then in many subsequent talks and notes [Thu80, Thu82, Thu89, KT90]. Thurston introduced the idea of traintracks to describe classes of simple closed curves on surfaces and used that idea to combinatorially describe the boundary of Teichmüller space. He also introduced the basic notions of circle packings and demonstrated their relevance to hyperbolic geometry. The limit sets of maximal cusp groups are all infinite circle packings of the Riemann sphere. These are just a few castoffs of Thurston's vast program in geometry and topology.

There have been very many results on the boundary since then, including McMullen's theorem [McM91] that the maximal cusp groups are dense in the boundary

of Bers' embedding of the Teichmüller space of a Riemann surface of finite type. As a result one can try to explore the boundary of Teichmüller space by calculating very many maximal cusps. Similarly, Canary, Culler, Hersonsky and Shalen prove in [CCHS03] that the maximal cusp groups are dense in the boundary of Schottky space.

In the manuscript [Wri87], the author explained numerical calculations of the cusps on the boundary of Maskit's version of the Teichmüller space of once-punctured tori, as well as some theoretical aspects of this calculation. The basics of that calculation now appear in the book *Indra's Pearls* [MSW02], and related material may be found in papers of Keen and Series, for example [KS92, KS93, KS94, KMS93].

In this paper, we have reworked the search for cusp groups in very elementary terms involving the existence of an arrangement of tangent circles (which we call the *circle web* of the group) and a set of Möbius transformations that maps some of the circles to others in a prescribed way. We will explain how maximal cusps on the boundary of the Schottky space of genus g may be described in this manner, and we will present several numerical examples of the geometry of these cusp groups. While leading up to higher genus theory and examples in Section 6, we review the theory of these circle webs for maximal cusps occurring on the boundary of Maskit's Teichmüller space of once-punctured tori in Section 2, on the space of pairs of punctured tori in Section 4, and Riley's slice of two-parabolic-generator groups in Section 5. We also present precise images of these maximal cusp groups for the first time.

In the course of reviewing the cusps on Maskit's $T_{1,1}$, we observed a striking parallel between the geometry of these cusp groups and that of the Doyle spiral circle hexagonal packings. In Section 3, we study spiral circle packings following some of the same techniques used for maximal cusp groups. We show that all the similarity factors of Doyle packings and their square grid analogues are algebraic numbers, and we present detailed calculations revealing a conjectural asymptotic pattern for these similarity factors, which is analogous to the cardioid shape of cusps on Maskit's $T_{1,1}$, proved in [Miy03].

Finally, we would like to extend deep thanks to the Isaac Newton Institute and the organizers Caroline Series, Makoto Sakuma and Yair Minsky for their support during the program on *Spaces of Kleinian Groups*, during which the bulk of this manuscript was prepared.

2. The first example: cusps on the boundary of Maskit's $T_{1,1}$

In [Mas74], Maskit gave a geometric method based on his combination theorems leading to a complex embedding of the Teichmüller space of a Riemann surface of finite

type. The specialization of this method to the case of a once-punctured torus yields a family of groups G_μ generated by two Möbius transformations of the form

$$a_\mu(z) = \mu + \frac{1}{z}, \qquad\qquad b(z) = z + 2.$$

We will sometimes denote a_μ by simply a. In addition, when we need to, we shall take the matrix realizations of these transformations to be

$$a_\mu = \begin{pmatrix} -i\mu & -i \\ -i & 0 \end{pmatrix}, \qquad\qquad b = \begin{pmatrix} 1 & 2 \\ 0 & 1 \end{pmatrix}.$$

Maskit proved that the set of values of μ with $\Im\mu > 0$ for which the group G_μ satisfies certain geometric conditions forms a model of the Teichmüller space of marked punctured tori. As a consequence, this set is a simply-connected domain in the upper half-plane, which we will simply refer to as $T_{1,1}$.

Our numerical calculation of this boundary was based on searching for cusps. For μ in $T_{1,1}$, all the elements of the group G_μ are hyperbolic (by which we mean not elliptic or parabolic; hence, this includes "loxodromic"), except for conjugates of powers of the words b and $abAB$. (We shall use the upper case convention to denote inverses of elements in our group. Thus, A and B are the inverses of a and b, respectively.) Cusps correspond to values of μ on the boundary where an additional word becomes "accidentally" parabolic.

Only one additional class of words in G_μ may become parabolic, and that class corresponds to a simple closed curve on the once-punctured torus. These words may be parametrized by rational numbers p/q. Additional details about this theory may be found in *Indra's Pearls* and the papers we have referenced above. There are several possibilities for this parametrization; for this paper, we will use the following.

Definition 2.1. For each fraction p/q in $\widehat{\mathbb{Q}} = \mathbb{Q} \cup \{1/0\}$, we define a word $w_{p/q}$ in the free group generated by a and b (with inverses A and B) by the following recursive rules:

(i) $w_{0/1} = A$ and $w_{1/0} = b$.

(ii) For any pair of fractions $p/q < h/k$ with $hq - kp = 1$, we have

$$w_{\frac{p+h}{q+k}} = w_{p/q} w_{h/k}.$$

The justification of this definition lies in the elementary theory of continued fractions, and we shall leave this to other sources. As a few examples, let us just mention

$$w_{5/8} = AAbAAbAbAAbAb, \qquad w_{1/15} = A^{15}b,$$
$$w_{-1/1} = AB \quad \text{(due to } w_{-1/1} w_{1/0} = w_{0/1}\text{)}, \qquad w_{-7/9} = (AB)^4 A (AB)^3 A.$$

In the group G_μ, the matrix entries of each word are polynomials in the complex variable μ. Thus, the condition that the word $w_{p/q}$ be parabolic is equivalent to a polynomial equation $\operatorname{tr} w_{p/q} = \pm 2$. The story of these trace polynomials is told partly in *Indra's Pearls* and in more detail in [KS92]. As a consequence of the analytic theory of Teichmüller space as constructed by Bers, there is precisely one solution of this trace equation lying on the boundary of $T_{1,1}$ and we shall denote this distinguished solution by $\mu(p/q)$. With the assumption that $\Im\mu > 0$, it turns out that in this case that solution satisfies the trace equation equal to 2. This is proved in [KS93] by an analysis of the 'p/q pleating rays' in $T_{1,1}$ which are shown to be curves terminating at the p/q cusp and along which the trace of the p/q word increases from 2 to ∞. The mirror image $\overline{T_{1,1}}$ of $T_{1,1}$ under complex conjugation has cusps on its boundary which are solutions of the other equation $\operatorname{tr} w_{p/q} = -2$; this happens precisely when q is odd. Minsky's work [Min99] on the space of pairs of punctured tori has established the fact that the mapping $p/q \mapsto \mu(p/q)$ continuously extends to an injective continuous map of $\mathbb{R}$ onto the boundary of $T_{1,1}$.

As explained in Chapter 9 of *Indra's Pearls*, the mapping $p/q \mapsto \mu(p/q)$ was used to numerically compute this boundary. It is easy to calculate by hand that $\mu(0/1) = 2i$, as well as various other values, for instance, $\mu(1/1) = 2+2i$ and $\mu(1/2) = 1+\sqrt{3}i$. To calculate other values of $\mu(p/q)$, we enumerate the Farey series of fractions of denominator at most D, for some large integer $D > q$, and we solve the trace equation $\operatorname{tr} w_{p/q} = 2$ for $\mu(p/q)$ by Newton's method using as the seed value $\mu(h/k)$ where h/k is the fraction preceding p/q in the Farey series. This is what we refer to as a *boundary tracing algorithm*. It turns out to be crucial to compute the trace polynomials in the most efficient recursive manner, and then to use a numerical approximation to the derivative that appears in the formula for Newton's method. Nonetheless, the convergence of this algorithm is quite fast. There are now other calculations of this and slices of other Teichmüller spaces by Komori-Sugawa-Wada-Yamashita (see [KS04, KSWY]); their program is based on a criterion for discreteness, rather than a search for cusps.

Now we turn to the most important part of this section, the geometry of the limit sets of the cusps. As an example, we take the $1/15$ cusp approximately given by

$$\mu(1/15) = 0.011278560612 + 1.958591030112\,i$$

corresponding to the word $A^{15}b$. As a maximal cusp, every simple closed curve on the corresponding Riemann surface may be shrunk to a puncture, and a consequence of this is that every component of the ordinary set is a circular disk stabilized by a Fuchsian subgroup of G_μ. There are several distinguished subgroups in G_μ. First, in all these groups we have that $\operatorname{tr} abAB = -2$, regardless of the value of μ. Therefore,

the subgroup H_1 generated by b and aBA has the property that $\operatorname{tr} b = \operatorname{tr} aBA = 2$ and $\operatorname{tr} b(aBA) = \operatorname{tr} abAB = -2$. The conditions $\operatorname{tr} u = \operatorname{tr} v = 2$, $\operatorname{tr} uv = -2$ always imply that the group generated by u and v is conjugate to the triply-punctured sphere group generated by

$$\begin{pmatrix} 1 & 2 \\ 0 & 1 \end{pmatrix}, \qquad \begin{pmatrix} 1 & 0 \\ -2 & 1 \end{pmatrix}.$$

In fact, in this case b and aBA are easily seen to be exactly those matrices. The limit set of H_1 is just the extended real line $\widehat{\mathbb{R}}$ bounding the lower half-plane D_1, which is a component of the ordinary set. For any element $g \in G_\mu$, we also have all the circles $g(\mathbb{R})$ belonging to the limit set of G_μ, bounding disks stabilized by gH_1g^{-1}.

In a cusp group, another family of circular disks appears. We consider the subgroup H_2 generated by $A^{15}b$ and $A(Ba^{15})a$. This also is seen to be a triply-punctured sphere group from the trace equations

$$\operatorname{tr} A^{15}b = \operatorname{tr} A(Ba^{15})a = 2,$$
$$\operatorname{tr} A(Ba^{15})aA^{15}b = \operatorname{tr} ABab = -2.$$

The limit set of H_2 is another circle bounding a disk D_2 in the ordinary set. The ordinary set of G_μ consists of the two families of disks $g(D_1)$ and $g(D_2)$ for all elements g of G_μ.

We emphasize a particular selection of these disks in Figure 1. We have relabelled D_1 as ε_0 and D_2 as δ_0. In addition, we have plotted certain images of ε_0 (all dark gray) and of δ_0 (all light gray) under elements of the group G_μ.

The numbering of the circles follows these rules:

$$a(\varepsilon_j) = \varepsilon_{j+1} \quad \text{for } 0 \le j \le 0; \qquad b(\varepsilon_j) = \varepsilon_{j+0} \quad \text{for } 0 \le j \le 1;$$
$$a(\delta_j) = \delta_{j+1} \quad \text{for } 0 \le j \le 15; \qquad b(\delta_j) = \delta_{j+15} \quad \text{for } 0 \le j \le 1.$$

We have stated these in a manner to show how they generalize to other cusp groups. This web of circles with mapping relations is enough to imply that the words b, $ABab$ and $A^{15}b$ are all parabolic. The reason is contained in a simple and obvious lemma.

Lemma 2.2. *A non-identity Möbius transformation that fixes each of a pair of tangent circles in the Riemann sphere is parabolic with unique fixed point equal to the tangent point.*

To start, the map b fixes both ε_0 and ε_1, which are tangent at ∞; this confirms b is parabolic. Secondly, we can follow the mapping relations to establish

$$ABab(\varepsilon_0) = ABa(\varepsilon_0) = AB(\varepsilon_1) = A(\varepsilon_1) = \varepsilon_0,$$
$$ABab(\delta_0) = ABa(\delta_{15}) = AB(\delta_{16}) = A(\delta_1) = \delta_0.$$

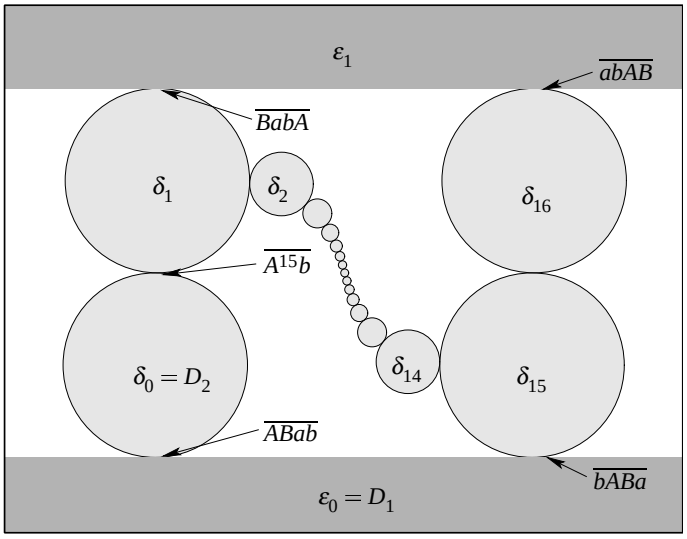

Figure 1: A chart of tangent circles in the ordinary set of the $1/15$ cusp group.

This establishes that *ABab* is parabolic with fixed point at the intersection point $\varepsilon_0 \cap \delta_0$. Finally, a similar argument proves that $A^{15}b$ fixes both δ_0 and δ_1, and hence its fixed point is $\delta_0 \cap \delta_1$. We have marked the fixed points of various words using the convention that $\overline{w}$ means the attractive fixed point of the Möbius map w.

The external tangency of the disks in the diagram is crucial to identifying this group as the $1/15$ cusp. The disk D_1 can be defined as that bounded by the unique circle passing through the points $\overline{ABab}$, $\overline{bABa}$ and $\overline{b}$ $(=\infty)$. Similarly, the disk D_2 can be defined as that bounded by the circle tangent to D_1 at $\overline{ABab}$ and passing through $\overline{A^{15}b}$. The other disks are defined by the mapping rules given above. Provided b, *ABab* and $A^{15}b$ are all parabolic, these disks will all be uniquely and well defined by these stipulations. Thus, there is such a circle web for any solution μ of the $1/15$ trace equation $\operatorname{tr} A^{15}b = \pm 2$. The particular solution $\mu(1/15)$ is the only solution with $\Im\mu > 0$ for which these disks are distinct and can be chosen to have disjoint interiors. (There is also one solution with $\Im\mu < 0$ which yields a mirror image circle web in the lower half-plane.)

To use the external tangency to establish that this cusp group is discrete and free, draw the orthogonal arcs in each disk between tangent points. The resulting arcs piece together to form four curves bounding "blobs" which are shown in Figure 2. The original web of circles is also shown in outline. Due to the mapping relations given above, the chain of 17 circles surrounding the hatched blob marked A is mapped

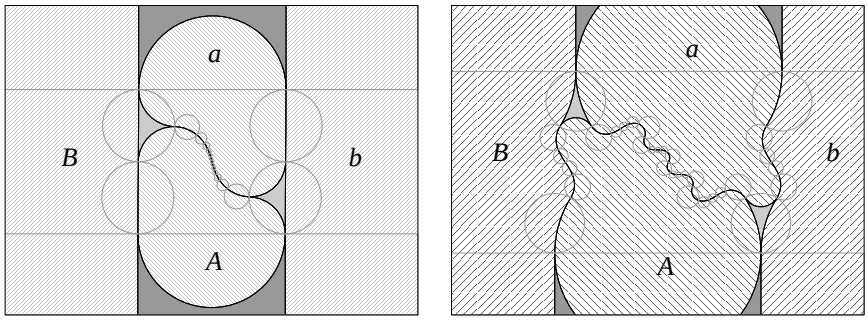

Figure 2: Drawing the orthogonal arcs in the circle web, we arrive at four Schottky *blobs*. The left frame is the $1/15$ cusp group; the right is the $5/26$ cusp group.

by the transformation a onto the chain of 17 circles surrounding the hatched blob labelled a. Since the arcs were chosen to be orthogonal to these circles, it follows that a maps the boundary of the A blob precisely onto the boundary of the a blob in such a way that the interior of the A blob is mapped onto the exterior of the a blob. The analogous argument shows that the transformation b maps the interior of the B blob (right hatched) onto the exterior of the b blob (also right hatched). We should point out that although the picture may not reveal this, the boundaries of both the B and b blobs consists of four separate circular arcs, two of which are half-lines passing through ∞.

The four blobs therefore satisfy exactly the mapping relations that define a Schottky group of genus two, except for the condition that their closures be disjoint. Much of Klein's combination theorem still applies, with the conclusions that the group generated by a and b is free and discontinuous, and that the common exterior of the four blobs, which consists of two dark gray circular (or "ideal") triangles (with one vertex at ∞) and two light gray circular triangles, is at least a subset of some fundamental region for the group. In fact, the four triangles do indeed form a fundamental region for the group, and the associated Riemann surface is a pair of triply-punctured spheres.

This example establishes the theme of this paper: defining cusp groups in terms of patterns of tangent circles with given mapping relations under given Möbius transformations. For the Maskit groups, the general mapping relations are a theorem of Keen and Series [KS92].

Theorem 2.3. *Given a fraction $0/1 \le p/q < 1/0$, for the p/q cusp group $G_\mu = \langle a, b\rangle$ on the boundary of Maskit's $T_{1,1}$ there are disjoint open disks ε_j, $0 \le j \le 1$, and δ_j, $0 \le j \le p+q$, such that*

$$a(\varepsilon_j) = \varepsilon_{j+1} \quad \textit{for } 0 \le j \le 0; \qquad b(\varepsilon_j) = \varepsilon_{j+0} \quad \textit{for } 0 \le j \le 1;$$
$$a(\delta_j) = \delta_{j+p} \quad \textit{for } 0 \le j \le q; \qquad b(\delta_j) = \delta_{j+q} \quad \textit{for } 0 \le j \le p.$$

Moreover, the following pairs of disks are externally tangent: $(\varepsilon_0, \varepsilon_1)$, (δ_j, δ_{j+1}) *for* $0 \le j \le p+q-1$, $(\varepsilon_0, \delta_0)$, $(\varepsilon_0, \delta_q)$, $(\varepsilon_1, \delta_p)$, $(\varepsilon_1, \delta_{p+q})$.

Conversely, given transformations a_μ *and* b *and disks* ε_j *and* δ_j *satisfying all these conditions,* $\langle a, b\rangle$ *is the* p/q *cusp group on Maskit's boundary.*

There is a similar statement for negative fractions $-p/q$, which can be deduced from the fact that $w_{-p/q}(a,b)$ is conjugate to $w_{p/q}(A,b)$. The more convoluted circle web for the $5/26$ cusp group is shown on the right in Figure 2. In this case, the chain of circles seems to consist of five chains of five circles each, which seems to correlate to the continued fraction expansion $\frac{1}{5+\frac{1}{5}}$ of $5/26$. Similar patterns may be perceived in the circle chains for more complicated fractions. We do not yet know a precise statement of how the circle web reveals the continued fraction expansion. For a very rough statement, we might hazard the following. For a fraction $p/q = \frac{1}{a_1 + \frac{r}{s}}$ with both p/q and r/s between 0 and 1, the circle chain of p/q appears to consist of a gentle spiral of a_1 mildly distorted copies of the r/s circle chain. Further analysis of this phenomenon may be found in work of Scorza [Sco].

3. Cusp groups and spiral circle packings

If we apply all powers of the transformation a to the original circles in the circle web shown in Figure 1, we obtain the two double spirals of disks depicted in Figure 3. Both spirals emanate from the repelling fixed point of a and flow into the attractive fixed point. There is a symmetry to this pattern in that each disk is tangent to exactly two disks of each shade. Locally, this packing of circles has the combinatorics of a square grid. Such a packing was called a *square grid circle packing* by Schramm in [Sch97], provided the circle which passes through the tangent points of a ring of four circles corresponding to one square in the grid is also orthogonal to those four circles. This is ever so slightly not true for the $1/n$ Maskit cusp groups. Nonetheless, the pattern is rigidly determined by a small subset of the mapping relations given in the previous section. In this section, we wish to compare these spiral circle packings against the bona fide square grid packings and the more common spiral hexagonal circle packings discovered by Peter Doyle and treated in [BDS94].

In general, the pattern for the $1/n$ cusp group is determined by the arrangement of the six disjoint disks ε_0, ε_1, δ_0, δ_1, η_0 and η_1, as shown in Figure 4. Here is the desired abbreviation of the mapping relations in Theorem 2.3.

Proposition 3.1. *For any complex number* μ *with imaginary part* $\tau = \Im\mu > 0$, *let* $a(z) = \mu + \frac{1}{z}$, $b(z) = z+2$, $\varepsilon_0 = \widehat{\mathbb{R}}$, $\varepsilon_1 = \widehat{\mathbb{R}} + i\tau$. *There is a unique value of* μ *such that we have circular disks* δ_0, δ_1, η_0, η_1 *satisfying the following properties:*

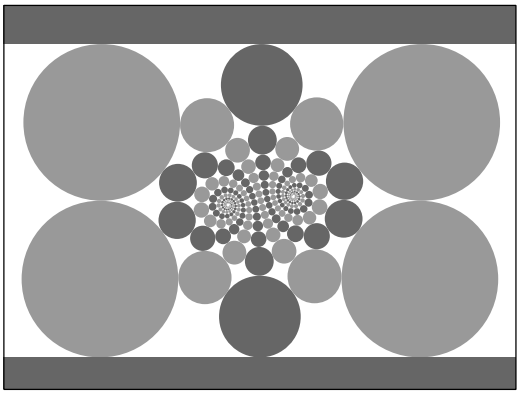

Figure 3: Spirals of circles in the 1/15 cusp group.

M0: *The six disks ε_j, δ_j, η_j have disjoint interiors, and the following circle pairs are externally tangent:*

$$(\varepsilon_0,\varepsilon_1),\quad (\delta_0,\delta_1),\quad (\eta_0,\eta_1),\quad (\delta_0,\varepsilon_0),\quad (\eta_0,\varepsilon_0),\quad (\delta_1,\varepsilon_1),\quad (\eta_1,\varepsilon_1).$$

M1: *$a(\delta_0)=\delta_1$, $a(\varepsilon_0)=\varepsilon_1$ and $a(\eta_0)=\eta_1$;*

M2: *$b(\varepsilon_j)=\varepsilon_j$ and $b(\delta_j)=\eta_j$ for $j=0,1$;*

M3: *$a^n(\delta_0)=\eta_0$;*

M4: *the disks $a^j(\delta_0)$ all have disjoint interiors.*

The group $\langle a,b\rangle$ is the $1/n$ Maskit cusp group.

Proof. Once again these conditions are sufficient to imply that b, $abAB$ and A^nb fix pairs of tangent circles and hence are all parabolic. The last condition completes proof on the basis of Theorem 2.3, since all the circles defined by $\delta_j = a^j(\delta_0)$ for $0 \le j \le n+1$ have disjoint interiors. □

One feature of these conditions is that, if we start at any circle in the pattern and follow the spiral arm that it lies on from one circle to the next, then after n steps (15 in the example shown in Figure 3) we arrive at a circle that is separated from the original circle by a single tangent circle on the other spiral. This feature can also be found in square grid and hexagonal (or Doyle) circle packings. In both of these cases, we will also assume that conditions **M0** and **M1** hold. We will replace **M2** by one of

H2: The pairs of circles (δ_0,ε_1) and (η_0,ε_1) are both externally tangent.

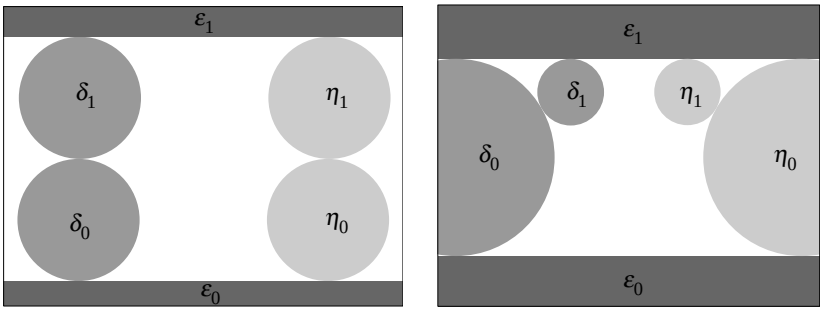

i) Maskit Diagram ii) Hex Packing Diagram

Figure 4: The cluster of six tangent circles for (i) the Maskit cusp groups and (ii) the hexagonal circle packing.

SG2: The circles passing through the tangent points of the two chains of four circles $(\varepsilon_0, \delta_0, \delta_1, \varepsilon_1)$ and $(\varepsilon_0, \eta_0, \eta_1, \varepsilon_1)$ are orthogonal to their respective chains of circles.

These are conditions on the geometry of the six circles, and yet both conditions lead to the existence of a second Möbius transformation $b(z)$. Before we come to that fact, we first examine the dependence of the circles δ_j, η_j on the original choice of circles ε_j. In the case of Doyle packings, this analysis overlaps with that found in [BDS94], although in this paper we start with the Möbius symmetry a of the Doyle flower rather than derive it.

Proposition 3.2. *Suppose ε_0 and ε_1 are circular disks which are externally tangent at the point z_0, and $a(z)$ is a Möbius transformation that maps ε_0 onto ε_1 and does not fix z_0. Then, for either choice of **H2** or **SG2** as an additional condition, there is at most one collection of circles δ_0, δ_1, η_0 and η_1 satisfying **M0**, **M1**, and the chosen third condition, as well as the topological condition that $a^{-1}(z_0)$ lies on the one component of the complement of the six disks that touches all six disks.*

The existence of such collections of circles depends on certain algebraic inequalities on μ.

Proof. We can conjugate by a Möbius map so that the tangent point becomes infinity, the inverse image of the tangent point under a becomes 0, and the bounding circles are now the horizontal straight lines $\widehat{\mathbb{R}}$ and $\widehat{\mathbb{R}} + i\tau$ for some $\tau > 0$. That is, ε_0 and ε_1 are now the shaded half-planes shown in either frame of Figure 4. After conjugation, we would have $a(0) = \infty$, which implies that the matrix of a is of the form $\begin{pmatrix} \alpha & \beta \\ -\beta^{-1} & 0 \end{pmatrix}$ or $a(z) = -\alpha\beta - \frac{\beta^2}{z}$. The interiors are mapped in the correct manner only if $-\beta^2$ is

positive. Then we can uniquely conjugate by a positive diagonal matrix $\begin{pmatrix} \gamma & 0 \\ 0 & \gamma^{-1} \end{pmatrix}$ so that a becomes the transformation $a(z) = \mu + \frac{1}{z}$ for some complex number μ with $\Im\mu > 0$. (Choose γ so that $-\gamma^4\beta^2 = 1$.) This shows that our starting pair ε_0, ε_1 in Figure 4 is perfectly general up to Möbius transformation.

The topological condition on $a^{-1}(\infty) = 0$ is designed to ensure that the disks δ_1 and η_1 lie "between" δ_0 and η_0 in the hexagonal packing case shown in Figure 4 (ii). In addition, the tangent points of δ_0 and η_0 to ε_0 must have opposite signs.

Let $\mu = \sigma + i\tau$ with $\tau > 0$. Let δ_0 be the circle tangent to $\varepsilon_0 = \widehat{\mathbb{R}}$ at x with radius $r \leq \tau/2$. Thus, the center of δ_0 is $x + ir$. The circle $\delta_1 = a(\delta_0)$ is then tangent to $a(\varepsilon_0) = \varepsilon_1$ at $a(x) = \mu + \frac{1}{x}$. The center c of δ_1 is symmetric in δ_1 to ∞, and therefore $a^{-1}(c)$ is symmetric in δ_0 to $a^{-1}(\infty) = 0$. Thus,

$$a^{-1}(c) = x + ir + \frac{r^2}{\overline{0 - x - ir}} = \frac{x^2}{x - ir}$$

which implies the center of δ_1 is

$$c = \mu + \frac{x - ir}{x^2} = \sigma + \frac{1}{x} + i(\tau - \frac{r}{x^2}).$$

Since δ_1 passes through $a(x) = \mu + \frac{1}{x}$, the radius of δ_1 is

$$|a(x) - c| = \frac{r}{x^2}.$$

Note that, if $x = 0$, then this radius is infinite, and δ_1 would be a half-plane which would not be disjoint from one of ε_0 or ε_1, a violation of **M0**. We conclude that $x \neq 0$. Furthermore, since δ_1 is required to be in the horizontal strip between 0 and μ, we deduce that $\frac{r}{x^2} \leq \frac{\tau}{2}$, or $x^2 \geq \frac{2r}{\tau}$.

The requirement that δ_0 and δ_1 be externally tangent is equivalent to

$$|c - (x + ir)| = r + \frac{r}{x^2},$$

or

$$\left| \left(\sigma + \frac{1}{x} - x \right) + i \left(\tau - r - \frac{r}{x^2} \right) \right| = r + \frac{r}{x^2}. \tag{3.1}$$

Now let us consider the third condition **SG2**. The common orthogonals to ε_0 and ε_1 are the vertical lines. Since δ_0 and δ_1 are bisected by the same vertical line, the real parts of their centers must be the same. That implies $\sigma + \frac{1}{x} = x$, or equivalently the quadratic equation

$$x^2 - \sigma x - 1 = 0, \tag{3.2}$$

which has one positive and one negative solution. From equation (3.1), the radius is

$$r = \frac{\tau}{2}\frac{x^2}{1+x^2}. \tag{3.3}$$

Thus, the choice of circles δ_0 and η_0 is uniquely determined. The inequalities that guarantee the existence of the collection of six circles as described come from the requirements that the δ_j's be disjoint from the η_j's. For each such pair of circles with centers c_1, c_2 and radii r_1, r_2 we derive an inequality from $|c1 - c2| \geq r_1 + r_2$. The inequalities are rather generous, even if they are tedious to write down.

On the other hand, consider the other choice of third condition **H2**, that δ_0 is also tangent to ε_1. This implies that the radius r of δ_0 is $\tau/2$ (half the width of the horizontal strip between ε_0 and ε_1). Then equation (3.1) becomes

$$\left|\left(\sigma + \frac{1}{x} - x\right) + i\frac{\tau}{2}\left(1 - \frac{1}{x^2}\right)\right| = \frac{\tau}{2}(1 + \frac{1}{x^2}).$$

Square both sides and simplify and we are left with

$$x^2 - \sigma x - 1 = \pm\tau.$$

Let's suppose the tangent points of δ_0 and η_0 to ε_0 are $x < 0$ and $y > 0$, respectively. The tangent points of δ_1 and η_1 to ε_1 must have real parts between x and y. This implies $\sigma + \frac{1}{x} > x$ and $\sigma + \frac{1}{y} < y$. Thus, by our equation and the condition $\tau > 0$, we have $\sigma x + 1 - x^2 = (\sigma + \frac{1}{x} - x)x = -\tau$, or $x^2 - \sigma x - \tau - 1 = 0$. Analogous reasoning implies that $y^2 - \sigma y - \tau - 1 = 0$. Thus, the tangent points of the circles δ_0 and η_0 to ε_0 are precisely the two solutions to

$$x^2 - \sigma x - \tau - 1 = 0, \tag{3.4}$$

one of which is positive and one of which is negative. This again establishes the uniqueness of the collection of six circles. Inequalities guaranteeing existence may again be derived from the disjointness of the δ_j's and η_j's. □

The next proposition reveals the second symmetry of these patterns of six circles. In fact, the existence of this symmetry is more general.

Proposition 3.3. *Let ε_j, δ_j, $j = 0, 1$, be circular disks with disjoint interiors such that the following pairs are externally tangent:*

$$(\varepsilon_0, \varepsilon_1), \quad (\delta_0, \delta_1), \quad (\delta_0, \varepsilon_0), \quad (\delta_1, \varepsilon_1).$$

Suppose there is a Möbius transformation $a(z)$ such that $a(\delta_0) = \delta_1$ and $a(\varepsilon_0) = \varepsilon_1$. Then there is a unique Möbius transformation $b(z)$ such that $b(\varepsilon_j) = \delta_j$ for $j = 0, 1$ and b commutes with a.

Proof. To begin with, we may conjugate so that $a(z) = z+1$ (the parabolic case) or so that $a(z) = \lambda z$ for some λ of absolute value at least 1. In the parabolic case, we may then conjugate by a translation so that ε_0, ε_1 are the circles of radius $\frac{1}{2}$ centered at 0 and 1, respectively. Since $a(\delta_0) = \delta_1$, it follows similarly that δ_0 and δ_1 are circles of radius $\frac{1}{2}$ centered at points c and $c+1$, respectively. Finally, since ε_0 and δ_0 are externally tangent, it follows that $|c| = 1$. Any commuting transformation is a translation, and the unique one that satisfies the statement is then $b(z) = z+c$.

In the non-parabolic case, we may conjugate by a similarity $z \mapsto \gamma z$ so that the disk ε_0 is then centered at 1. Let r,s be the radii of ε_0, δ_0, respectively. Since $\varepsilon_1 = a(\varepsilon_0)$, the center of ε_1 is λ and the radius is $|\lambda| r$. Since ε_0 is tangent to ε_1, we conclude that

$$r = \frac{|\lambda - 1|}{|\lambda| + 1}.$$

Let κ be the center of the disk δ_0; since $\delta_1 = a(\delta_0)$ the center and radius of δ_1 are $\kappa\lambda$ and $|\lambda| s$, respectively. A similar argument to that for the ε's based on the tangency of δ_0 and δ_1 proves that

$$s = \frac{|\kappa\lambda - \kappa|}{|\lambda| + 1} = |\kappa| r.$$

This establishes that the similarity $b(z) = \kappa z$ maps ε_j to δ_j for $j = 0, 1$. The uniqueness follows from the fact that any transformation that commutes with a nontrivial similarity $a(z) = \lambda z$ is another similarity of the same form. □

Remark 3.4. In the non-parabolic case of Proposition 3.3 where the transformations have the form $a(z) = \lambda z$ and $b(z) = \kappa z$ after conjugation, the similarity factors are related by the equation

$$\frac{|\lambda - 1|}{|\lambda| + 1} = \frac{|\kappa - 1|}{|\kappa| + 1}$$

which comes from the calculation of the radius of ε_0 by using the tangency of ε_0 to $\varepsilon_1 = a(\varepsilon_0$ and $\delta_0 = b(\varepsilon_0)$.

With the two transformations a and b, we can extend our original six circles by considering all image circles $a^n b^m(\varepsilon_0)$ for integers n, m and thereby obtain the corresponding circle packing. The extension of the cluster in Figure 4 (ii) is shown in Figure 5. The surprise is that all the circles belong to the same double spiral. That is, all the circles are $a^n(\varepsilon_0)$ for all integers n. We have shaded the disks $a^j(\delta_0)$ for $0 \le j \le 15$ and $A^j(\eta_1)$ for $0 \le j \le 16$ differently from the rest to show how the spiral arm nestles against itself. In particular, after 16 steps from any given circle on the spiral arm, we come to a circle tangent to the original circle.

To highlight the combinatorics of this circle packing, we give each disk one of 16 different shades in succession along the spiral arm. The shades align themselves in 16

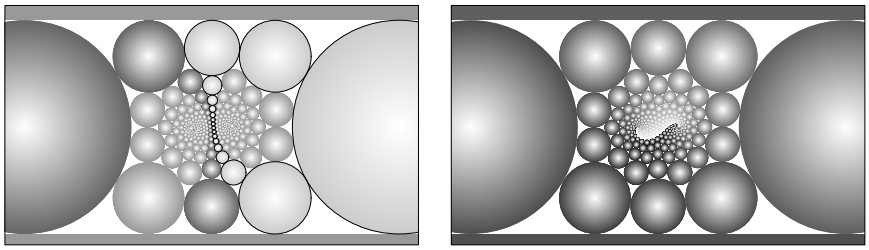

Figure 5: A spiral hexagonal circle packing. All the circles belong to one infinite double spiral generated by a Möbius transformation a. After 16 steps along this spiral, we arrive at a circle tangent to the original circle. The second picture shows the circles shaded with a different choice of exactly 16 shades, showing how the circles align themselves into spirals invariant under a second Möbius transformation b.

new spiral arms shown in Figure 5. The second Möbius transformation b moves the circles along these new spirals. In fact, we have $a^{16} = b$.

A diagram of the basic Doyle "flower" for the spiral packing of Figure 5 after conjugation is shown in Figure 6. We have marked the points 1, λ, λ^2, κ and κ/λ to show the arrangement of the similarity factors we have discussed.

We now introduce the analogue of conditions **M3** and **M4** for these circle packings.

Definition 3.5. We say the family of disks $\{a^n b^m(\varepsilon_0)\}$ is *coherent* if any pair of disks are either the same or have disjoint interiors.

In the parabolic case, all the disks have disjoint interiors. In the non-parabolic case, the coherent Doyle packings were analyzed in [BDS94], and the coherent square grid packings are treated in [Sch97]. In these cases, coincidence of the circles amounts to an equation of the form

$$a^q = b^p \tag{3.5}$$

for some pair of integers (p,q), not both zero. Generally, we will restrict ourselves to the case where the multipliers of a and b are of absolute value at least 1, and so the integers (p,q) are both nonnegative.

In [BDS94], it is proved there is a unique coherent Doyle packing satisfying equation (3.5) for any such integer pair (p,q) with $p \neq 0$, excluding a few small ones such as $(1,1),(1,2),(2,1),(2,2)$. The uniqueness is based on a circle packing rigidity theorem of Schramm. The rigidity of the square grid packings is treated in [Sch97]. We would like to make one small observation that might not have been noticed before.

Proposition 3.6. *The similarity factors of coherent spiral Doyle packings and coherent spiral square grid packings are algebraic numbers.*

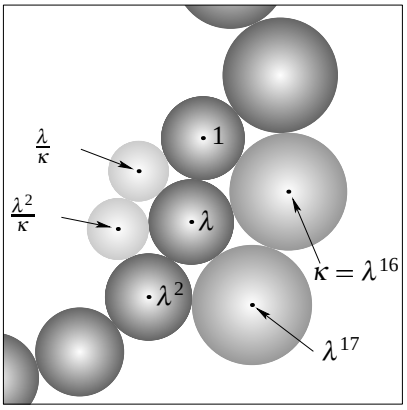

Figure 6: A Doyle fbwer with centers marked and labelled in terms of the similarity factors λ and κ. By repeatedly applying a to the circle centered at 1 until after 16 steps we arrive back at the circle centered at $\kappa = \lambda^{16}$.

Proof. First, let us conjugate the transformations so that $a(z) = \mu + 1/z$ again, and so that $\varepsilon_0 = \widehat{\mathbb{R}}$ and $\varepsilon_1 = \mu + \widehat{\mathbb{R}}$. The multiplier λ of a satisfies $\sqrt{\lambda} + 1/\sqrt{\lambda} = -i\mu$, by considering the trace of a. In Proposition 3.2, we have determined the two choices for δ_0. The tangent point x of δ_0 to ε_0 satisfies the quadratic equation (3.4) in the Doyle case, and (3.2) in the square grid case. Picking one of these solutions x, the radius of δ_0 is $\tau/2$ in the Doyle case and given by (3.3) in the square grid case.

To determine the second transformation b, we note that it shares fixed points with a, which are given by

$$z_1, z_2 = \frac{1}{2}(\mu \pm \sqrt{\mu^2 + 4}).$$

Suppose that the signs are chosen so that

$$\frac{a(z) - z_1}{a(z) - z_2} = \lambda \, \frac{z - z_1}{z - z_2}.$$

Since $a(0) = \infty$, this means $z_2 = \lambda z_1$. Then the transformation b is given by

$$\frac{b(z) - z_1}{b(z) - z_2} = \kappa \, \frac{z - z_1}{z - z_2}.$$

We can determine the multiplier κ of b by noting that b maps the tangent point of ε_0 and ε_1, which is ∞, to the tangent point z_0 of δ_0 and δ_1. This means we have

$$\kappa = \frac{z_0 - z_1}{z_0 - z_2}.$$

The tangent point in the square grid case is easy to determine:

$$z_0 = x + 2ir = x + i\tau \frac{x^2}{1 + x^2}.$$

The centers c_0, c_1 and radii r_0, r_1 of δ_0 and δ_1 in either case were determined in the proof of Proposition 3.2. Thus, the tangent point can be determined on the line segment between c_0 and c_1 as $z_0 = \frac{r_1 c_0 + r_0 c_1}{r_0 + r_1}$. After a small amount of algebra, we find the tangent point in the Doyle case to be

$$z_0 = \frac{x(2+\mu x)}{1+x^2}.$$

Since σ, τ lie in $\mathbb{Q}(\mu, \overline{\mu}, i) \subset \mathbb{Q}(\sqrt{\lambda}, \sqrt{\overline{\lambda}}, i)$, and x lies in a quadratic extension of $\mathbb{Q}(\sigma, \tau)$, we see that κ lies in a solvable algebraic extension of at most degree 16 of $\mathbb{Q}(\lambda)$. The coherence equation $\lambda^q = \kappa^p$ then may be simplified to a polynomial equation for λ over $\mathbb{Q}$. □

We shall give some examples of the algebraic determination of these similarity factors. The first is the case of a Doyle packing with $p = 1$, $q = 4$, which is known as the Brooks spiral (see [Ste, Bro85]). In the configuration of Figure 4 (ii), we should have $\varepsilon_4 = a^4(\varepsilon_0) = \delta_0$, which is tangent to ε_0 and ε_1. This implies $\varepsilon_2 = a(\varepsilon_1)$ is tangent to $\varepsilon_{-1} = A(\varepsilon_0)$ and ε_{-2}. That inspires the following calculation.

Lemma 3.7. (i) *The image $\varepsilon_{-1} = A(\varepsilon_0)$ is the circle of radius $\frac{1}{2\tau}$ centered at $\frac{i}{2\tau}$.*

(ii) *The image $\varepsilon_2 = a(\varepsilon_1)$ is the circle of radius $\frac{1}{2\tau}$ centered at $\mu - \frac{i}{2\tau}$.*

Proof. Let ε_{-1} have center c and radius r. Since c is symmetric with ∞ in ε_{-1}, we will have $a(c)$ symmetric with $a(\infty) = \mu$ in ε_0. Thus, $a(c) = \overline{\mu}$, and hence $c = A(\overline{\mu}) = \frac{1}{\overline{\mu} - \mu} = \frac{i}{2\tau}$. Since ε_{-1} is tangent to ε_0 at $A(\infty) = 0$, the radius of ε_{-1} is $\frac{1}{2\tau}$.

For the second part, note that the order two rotation $r(z) = \mu - z$ conjugates a into A, that is, $rar = A$. Thus, $\varepsilon_2 = a^2(\varepsilon_0) = rA^2 r(\varepsilon_0) = rA^2(\varepsilon_1) = r(\varepsilon_{-1})$. Hence, ε_2 has center $\mu - \frac{i}{2\tau}$ and radius $\frac{1}{2\tau}$. □

From Lemma 3.7, the disks ε_{-1} and ε_2 are tangent if and only if $|\mu - \frac{i}{2\tau} - \frac{i}{2\tau}| = 2\frac{1}{2\tau}$, which simplifies to $|\mu| = \sqrt{2}$.

Suppose now the center of ε_{-2} is c. Then $a(c)$ is symmetric with $a(\infty) = \mu$ in ε_{-1}. Thus,

$$a(c) = \frac{i}{2\tau} + \frac{(1/(2\tau))^2}{\overline{\mu - \frac{i}{2\tau}}} = \frac{\overline{\mu}}{1 - 2i\tau\overline{\mu}}.$$

Since $a(c) = \mu + \frac{1}{c}$ and $\mu\overline{\mu} = |\mu|^2 = 2$, we can simplify the above to find $c = -\overline{\mu} - \frac{i}{2\tau}$. Since ε_{-2} is tangent to ε_1 and $\Im(-\overline{\mu}) = \Im\mu$, we see the radius is $\frac{1}{2\tau}$. The tangency between ε_{-2} and ε_2 now yields

$$\left| \mu - \frac{i}{2\tau} - \left(-\overline{\mu} - \frac{i}{2\tau} \right) \right| = \frac{1}{\tau}$$

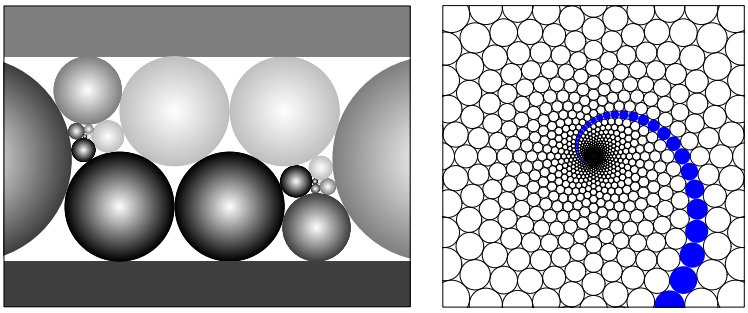

Figure 7: Two Doyle spirals: The left frame is the Brooks spiral, corresponding to $p = 1$, $q = 4$. The right frame is a portion of a pattern explored by R. Weedon. It corresponds to $p = 20$, $q = 40$.

This reduces to $2|\sigma| = |\mu + \overline{\mu}| = \frac{1}{\tau}$. Inserting this into $\sigma^2 + \tau^2 = 2$, it is a simple matter to solve for σ and τ, and we find

$$\mu(1,4) = \frac{\sqrt{3}-1}{2} + i\,\frac{1+\sqrt{3}}{2}.$$

The similarity factor λ may then be found by solving $-i\mu = \sqrt{\lambda} + \frac{1}{\sqrt{\lambda}}$, although the exact expression is rather messy. Numerically, we have

$$\begin{aligned} \mu(1,4) &= 0.366025403784440 + 1.36602540378444\,i, \\ \lambda &= 0.194235974222535 + 1.61161245101347\,i, \\ |\lambda| &= 1.62327517874938. \end{aligned}$$

The Brooks spiral is shown in Figure 7, colored with 4 shades in succession. One can detect the progression of the spiral arm by observing that ε_j and ε_{j+1} always have distinct shades, while ε_j and ε_{j+4} are always tangent disks of the same shade.

Remark 3.8. The requirements that ε_2 and ε_{-1} lie in the strip between ε_0 and ε_1 are therefore equivalent with the condition $\tau = \Im\mu \geq 1$. If we require that ε_2 and ε_{-1} also have disjoint interiors, from the above lemma we may derive the inequality

$$|\mu| \geq \sqrt{2}.$$

This gives us some preliminary estimates for values of μ corresponding to coherent circle packings of either type. The same estimates apply to Maskit's $T_{1,1}$ as well.

A more symmetric version of the equations determining λ and κ may be extracted from Proposition 3.6 (see [BDS94]). This version would be the coherence equation

together with the tangency equations.

$$\frac{|\lambda-1|}{|\lambda|+1} = \frac{|\kappa-1|}{|\kappa|+1} = \frac{|\lambda-\kappa|}{|\lambda|+|\kappa|}. \tag{3.6}$$

R. Weedon of the United Kingdom has explored the families of Doyle packings where $q = p$ or $q = 2p$. A general observation in [BDS94] is that when $r = \mathrm{GCD}(p,q) > 1$ there is a rotational symmetry of order r in the corresponding Doyle packing. That is, $\lambda^{p/r}\kappa^{-q/r}$ is an r-th root of unity. For $q = p$ the the equations (3.6) and (3.5) may be solved to yield

$$w = \tan^2\frac{\pi}{p} + \sec\frac{\pi}{p}, \qquad\qquad \ell = w + \sqrt{w^2-1}.$$

For $q = 2p$, the solution may be obtained by the following recipe.

$$c = \cos\frac{\pi}{p}, \qquad w = \sqrt{\frac{\sqrt{5+4c}-2c-1}{2}}, \qquad \ell = \frac{1+w}{c+w^2},$$

In both cases, the multiplier is given by $\lambda = \ell\exp\frac{i\pi}{p}$. The pattern for $p = 20$, $q = 40$ is shown in Figure 7.

The complexity of the equations in general seems to make exact formulas difficult to obtain. However, using Newton's method again, it is possible to numerically solve the algebraic equations derived in Proposition 3.6. We made use of several Maple procedures to accomplish this. First, two procedures `multiplier` and `similar` calculate the corresponding λ and κ to a given μ; these are simply a matter of extracting square roots carefully. The iterative part comes in solving the coherence equation

$$L_{p,q}(\mu) = \texttt{multiplier}(\mu)^q - \texttt{similar}(\mu)^p = 0.$$

Unlike the case of the Maskit trace polynomials, this equation is only a real analytic function of μ, not complex analytic. We use a two-dimensional real Newton's method to solve for the solution μ. We define a two-dimensional vector valued function:

$$F\begin{pmatrix}\sigma\\ \tau\end{pmatrix} = \begin{pmatrix}\Re L_{p,q}(\sigma+i\tau)\\ \Im L_{p,q}(\sigma+i\tau)\end{pmatrix}$$

One pass of Newton's method consists of starting with a seed value $\begin{pmatrix}\sigma_0\\ \tau_0\end{pmatrix}$, numerically computing the jacobian matrix

$$J_F = \begin{pmatrix}\frac{\partial F_1}{\partial\sigma} & \frac{\partial F_1}{\partial\tau}\\ \frac{\partial F_2}{\partial\sigma} & \frac{\partial F_2}{\partial\tau}\end{pmatrix}$$

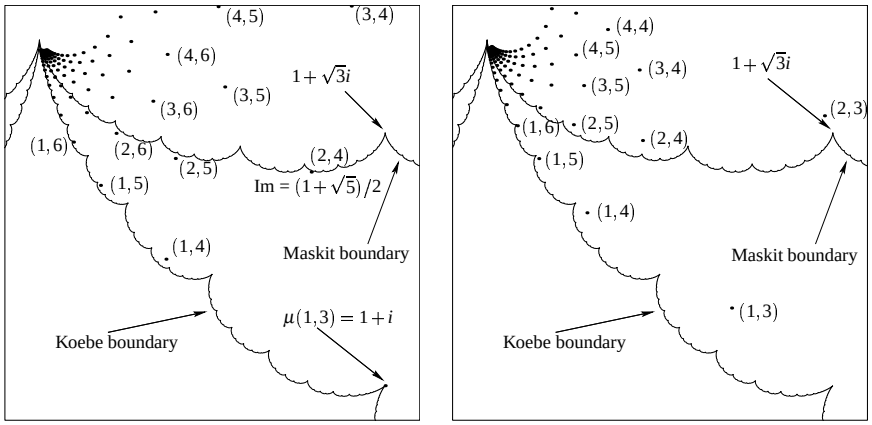

Figure 8: Chart of the constants μ for the $\langle p,q\rangle$ coherent Doyle packings (left) and square grid packings (right). Superimposed on the plot are traces of Maskit's boundary of $T_{1,1}$ and of the boundary of the Koebe slice of groups $\langle a,b\rangle$ with *abAB* parabolic and *b* elliptic of order 2.

by means of some very small increments in σ and τ, and then solving the linear system $J_F\begin{pmatrix}\Delta\sigma\\ \Delta\tau\end{pmatrix} = -F\begin{pmatrix}\sigma_0\\ \tau_0\end{pmatrix}$ for the change in σ, τ. The refined approximation of the solution is then $\sigma_0+\Delta\sigma$, $\tau_0+\Delta\tau$. With a good initial guess, the process produces a solution very quickly.

By moderate diligence, we compiled the constants $\mu(p,q)$ for $p\le 6$ and $q\le 20$ for both the Doyle and the spiral square grid packings. We have displayed these values for the Doyle packings in Figure 8. Typically, ten digits of accuracy requires less than ten Newton passes, once a good seed value has been found. The chart shows that the values of $\mu(2,q)$ follow closely the shape of the Maskit $T_{1,1}$ boundary (which is plausible since both circle packings are composed of two double spirals), while the values of $\mu(1,q)$ follow the shape of the boundary of another deformation space of Koebe groups (see [Par95]; Wada communicated that this is essentially the same as the Riley slice).

The chart makes clear that the constants $\mu(p,q)$ have a strong asymptotic pattern. We may elucidate this pattern by first computing $\sqrt{\lambda}$ from $\sqrt{\lambda}+\frac{1}{\sqrt{\lambda}} = -i\mu$ (so that λ is the multiplier), and then plotting the expression $\frac{i}{1-\sqrt{\lambda}}$ for all the data points shown above. Figure 9 shows that the points for Doyle packings lie on an approximate hexagonal lattice, while those for the square grid packings lie on an approximate

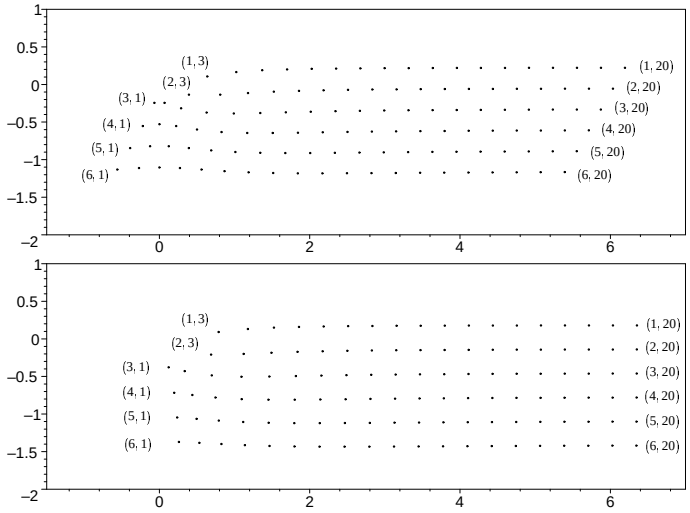

Figure 9: Plot of $\frac{i}{1-\sqrt{\lambda}}$ for $\sqrt{\lambda}+\frac{1}{\sqrt{\lambda}} = -i\mu(p,q)$ for the Doyle packings (top) and square grid packings (bottom). The points follow asymptotic hexagonal and square lattices , respectively, edge length $\frac{1}{\pi}$. Some points are labelled with the corresponding (p,q). The value of q increases from left to right, and the value of p increases downward.

square lattice. In fact, the asymptotic formulas appear to be

$$\frac{i}{1-\sqrt{\lambda(p,q)}} = \frac{i}{2} + \frac{1}{\pi}(q - p\,e^{\pi i/3}) \qquad (Doyle)$$

$$\frac{i}{1-\sqrt{\lambda(p,q)}} = \frac{3i}{2\pi} + \frac{1}{\pi}(q - p\,i) \qquad (SquareGrid)$$

For large p and q, only a few passes of Newton's method are required to obtain the value $\mu(p,q)$ to high precision from this seed value. In [Wri87], a similar asymptotic formula for the Maskit cusps $\mu(1/n)$ was conjectured based on algebraic manipulation of the corresponding trace polynomials. In the above form, this asymptotic formula would be expressed as

$$\frac{i}{1-\sqrt{\lambda(1/n)}} = \frac{(\pi-4)i}{2\pi} + \frac{n}{\pi} \qquad (Maskit)$$

The main term (and probably more) was established by Miyachi in [Miy02, Miy03]. It's possible similar geometric methods could be used to establish the asymptotics of the coherent circle packings.

4. Double cusp groups on the space of pairs of punctured tori

For the remainder of the paper, we concentrate on the problem of maximal cusps on the boundary of deformation spaces. In this section, we consider the space of quasifuchsian groups $\langle a, b\rangle$ with $\operatorname{tr} abAB = -2$ which represent a pair of once-punctured tori. We'll refer to this as PPT space for brevity. One choice of complex parameters for this space is the pair of traces $(\operatorname{tr} a, \operatorname{tr} b)$. This is a two complex-dimensional space, and there is consequently a much more complicated boundary. In the interior of this space, all the words in G are hyperbolic except for conjugates of powers of $abAB$. A maximal cusp group on the boundary has two additional classes of words becoming accidentally parabolic, corresponding to a simple closed curve on each torus being pinched to a point. The two accidentally parabolic words are again conjugate to powers of the words of the form we defined in Section 2, $w_{p/q}$ and $w_{r/s}$ for some pair of different fractions p/q, r/s. Given such fractions, we may seek a maximal cusp by solving the two algebraic equations

$$\operatorname{tr} w_{p/q} = \pm 2, \qquad\qquad \operatorname{tr} w_{r/s} = \pm 2.$$

for solutions $(\operatorname{tr} a, \operatorname{tr} b)$ lying on the boundary of quasifuchsian space. There will be one solution corresponding to pinching the p/q curve on one torus and the r/s curve on the other torus, and a second solution corresponding to pinching the r/s curve on the first torus and the p/q curve on the second. By Theorem III of [KMS93], these two points are represented by anticonformally conjugate groups in $\mathrm{PSL}(2,\mathbb{C})$.

One might suspect that the extra degree of freedom makes this task significantly more difficult than the problem of finding cusps for Maskit's $T_{1,1}$. However, there is a very useful, labor-saving fact: every maximal cusp on the boundary of quasifuchsian space is conjugate to a maximal cusp on the boundary of Maskit's $T_{1,1}$ or its mirror image $\overline{T_{1,1}}$ under complex conjugation. Essentially, no new groups need to be unearthed to calculate the maximal cusps for quasifuchsian space. We will give only a few examples to show how to calculate cusps on quasifuchsian space, and we shall again emphasize the circle web that reveals the limiting Schottky nature of these groups.

The key to finding the cusp corresponding to the pair fractions $(p/q, r/s)$ lies in the Farey tessellation diagram shown in Figure 9.7 of *Indra's Pearls*, which gives the structure of the rational numbers relative to the process of the Farey addition $\frac{p+r}{q+s}$ of fractions p/q, r/s which are Farey neighbors, meaning that $rq - sp = \pm 1$. Rather than reproduce all the Farey theory explained in *Indra's Pearls*, we shall just show a chart indicating the use of Farey addition to move from one fraction to the next.

As a first example, we take the fractions $(5/8, -7/9)$. The fraction $-q/p$ is something like the "antipodal" fraction to p/q, so that this pair, while not antipodal, is in

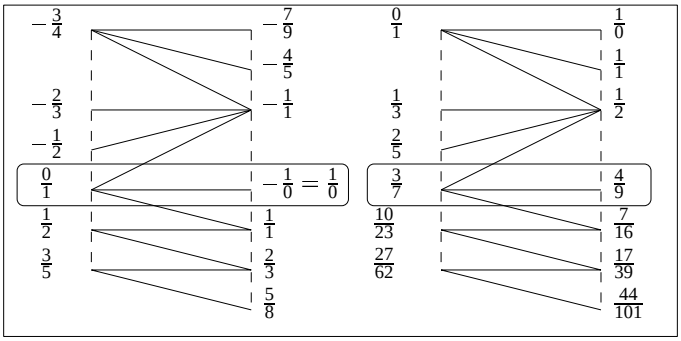

Figure 10: Chart of the Farey steps from the fraction $-7/9$ to $5/8$, and the computation of the analogous Maskit fraction $44/101$..

some sense spread far apart. In *Indra's Pearls*, we show some antipodal Fibonacci fraction pairs approximating a doubly degenerate boundary group. We begin by charting the edges in the Farey tessellation separating the two fractions as shown in Figure 10.

Each roughly horizontal edge in the chart connects a pair of fractions $(p/q, r/s)$ with $rq - sp = \pm 1$, i.e. Farey neighbors. The change from one pair of fractions to the next as we follow the chart from top to bottom consists of a single Farey addition (upward or downward). This chart is always uniquely determined by the original pair of fractions. To construct the righthand chart, we consider the same sequence of "pivots" or edges in the Farey tessellation starting from the edge between $0/1$ and $1/0$, with $1/0$ positioned at one of the original fractions (in this case $-7/9$). At the end of the sequence of moves, in the position of the other fraction in the original pair there will be an equivalent fraction h/k, defining a Maskit cusp $\mu = \mu(h/k)$ for which $G_\mu = \langle a_0, b_0 \rangle$ has the properties that $w_{1/0} = B$ and $w_{h/k}$ are both parabolic. Now we turn to the fractions in the righthand chart that are in the same positions as $0/1$ and $1/0$ in the lefthand chart (both pairs are circled). In this example, we construct a group $\langle a, b \rangle$ such that

$$\operatorname{tr} a = \operatorname{tr} w_{3/7}(a_0, b_0), \qquad \operatorname{tr} B = \operatorname{tr} w_{4/9}(a_0, b_0), \qquad \operatorname{tr} aB = \operatorname{tr} w_{7/16}(a_0, b_0).$$

Since $w_{3/7}$ and $w_{4/9}$ are generators of G_μ, it follows that the new group is conjugate to G_μ. This new group will have the property that $\operatorname{tr} w_{-7/9}(a, b) = \operatorname{tr} B_0 = 2$ and $\operatorname{tr} w_{5/8}(a, b) = \operatorname{tr} w_{44/101}(a_0, b_0) = \pm 2$, and thus corresponds to a maximal cusp, associated to $(\frac{5}{8}, -\frac{7}{9})$ or $(-\frac{7}{9}, \frac{5}{8})$. The same argument succeeds for any pair of distinct fractions.

An easier way around the arithmetic is to carry out these operations inside the

group $\mathrm{SL}_2(\mathbb{Z})$. For each pair of fractions on an edge $(\frac{p}{q}, \frac{r}{s})$ from left to right, associate the matrix $\begin{pmatrix} r & s \\ p & q \end{pmatrix}$, which must have determinant ± 1. Multiply the top row by -1 if the determinant is -1. Suppose A is the matrix so obtained for the top edge of the chart and B is the matrix for the bottom edge of the chart. Then there is a matrix U in $\mathrm{SL}_2(\mathbb{Z})$ such that $UA = B$. The equivalent fraction we calculated above is just the top row of this matrix $U = BA^{-1} = \begin{pmatrix} h & k \\ * & * \end{pmatrix}$. The fractions $3/7$, $4/9$ that were used at the end to find the traces of the desired maximal cusp group come from the rows of the matrix A^{-1}.

To continue with our example, our boundary tracing program computes the Maskit cusp

$$\mu(44/101) = 0.88884237349 + 1.63202851011i.$$

From that value, we can calculate

$$\begin{aligned} \operatorname{tr} w_{3/7} &= 1.5720620876 - 0.6328874943i, \\ \operatorname{tr} w_{4/9} &= 1.4493809001 + 1.4142149587i, \\ \operatorname{tr} w_{7/16} &= 1.5223946854 + 0.9431138430i. \end{aligned}$$

Formulas such as those given in *Indra's Pearls* may now be used to generate the matrices a, b of the maximal cusp group.

We are interested in the chains of circular disks that occur in the ordinary set of the maximal cusp group associated to $(p/q, r/s)$. The same reasoning as in Section 2 shows that the group generated by *ABab* and $w_{p/q}(a,b)$ is a fuchsian triply-punctured sphere group. This group stabilizes a disk passing through the fixed points of *ABab* and $w_{p/q}(a,b)$ and stabilized by the commutator *ABab* (a convenient third condition since the commutator is usually easy to compute). That gives us one disk $D_1 = \delta_0$ in the ordinary set, and we obtain the circle chain by applying a and b according to the dynamical rules stated in Theorem 2.3. However, the same process applied to the disk $D_2 = \varepsilon_0$ stabilized by *ABab* and passing through the fixed point of $w_{r/s}(a,b)$ gives a second chain for the fraction r/s. A corollary of the Keen-Series Theorem 2.2 is that the two chains link up in a meaningful way. First, we will state the pattern only for positive fractions.

Theorem 4.1. *Given a pair of distinct fractions $0/1 \le p/q, r/s \le 1/0$, for the p/q, r/s cusp group $G = \langle a, b\rangle$ on the boundary of PPT space there are disjoint open disks*

ε_j, $0 \le j \le r+s$, and δ_j, $0 \le j \le p+q$, such that

$$a(\varepsilon_j) = \varepsilon_{j+r} \quad \text{for } 0 \le j \le s; \qquad b(\varepsilon_j) = \varepsilon_{j+s} \quad \text{for } 0 \le j \le r;$$
$$a(\delta_j) = \delta_{j+p} \quad \text{for } 0 \le j \le q; \qquad b(\delta_j) = \delta_{j+q} \quad \text{for } 0 \le j \le p.$$

Moreover, the following pairs of disks are externally tangent:

- (δ_j, δ_{j+1}) *for* $0 \le j \le p+q-1$;
- $(\varepsilon_j, \varepsilon_{j+1})$ *for* $0 \le j \le r+s-1$;
- $(\varepsilon_0, \delta_0)$, $(\varepsilon_r, \delta_p)$, $(\varepsilon_s, \delta_q)$, $(\varepsilon_{r+s}, \delta_{p+q})$.

Conversely, given transformations a, b, disks ε_j, δ_j satisfying all these conditions, $\langle a, b\rangle$ is conjugate to the $(\frac{p}{q}, \frac{r}{s})$ cusp group.

Unlike Theorem 2.3 where the question of existence is a little more subtle, this theorem is simply an exercise in the arithmetic of $\mathrm{SL}_2(\mathbb{Z})$. The third set of tangencies listed are at the commutator fixed points $\overline{ABab}$, $\overline{BabA}$, $\overline{bABa}$ and $\overline{abAB}$ (respectively).

Since our examples will involve some negative fractions, we now state the modification necessary for one negative fraction.

Theorem 4.2. *Given a pair of fractions $0/1 \le p/q \le 1/0$, $-1/0 < -r/s < 0/1$, for the p/q, r/s cusp group $G = \langle a, b\rangle$ on the boundary of PPT space there are disjoint open disks ε_j, $0 \le j \le r+s$, and δ_j, $0 \le j \le p+q$, such that*

$$a(\varepsilon_j) = \varepsilon_{j+r} \quad \text{for } 0 \le j \le s; \qquad B(\varepsilon_j) = \varepsilon_{j+s} \quad \text{for } 0 \le j \le r;$$
$$a(\delta_j) = \delta_{j+p} \quad \text{for } 0 \le j \le q; \qquad b(\delta_j) = \delta_{j+q} \quad \text{for } 0 \le j \le p.$$

Moreover, the following pairs of disks are externally tangent:

- (δ_j, δ_{j+1}) *for* $0 \le j \le p+q-1$;
- $(\varepsilon_j, \varepsilon_{j+1})$ *for* $0 \le j \le r+s-1$;
- $(\varepsilon_s, \delta_0)$, $(\varepsilon_{r+s}, \delta_p)$, $(\varepsilon_0, \delta_q)$, $(\varepsilon_r, \delta_{p+q})$.

The converse holds as in Theorem 4.1.

Figure 11 shows the circle chains for the $5/8$, $-7/9$ maximal cusp group. The δ circle chain for $5/8$ (lightly shaded) and the ε chain for $-7/9$ (darker) have been numbered according to the above theorem.

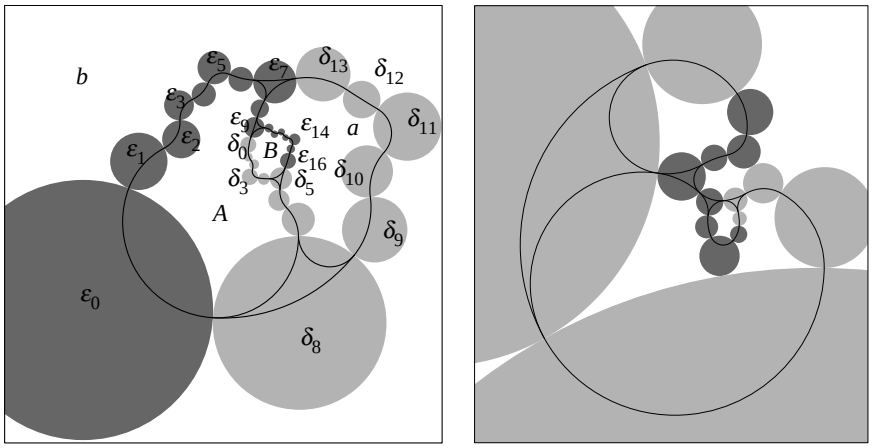

Figure 11: Chains of circles in maximal cusp groups on the boundary of quasifuchsian space. Left frame: the $(\frac{5}{8}, -\frac{7}{9})$ group; right frame: the $(\frac{3}{4}, \frac{1}{5})$ group.

Again we connect all pairs of tangent points on a given disk by orthogonal arcs to the bounding circle. These arcs piece together into four simple closed curves bounding the Schottky blobs. The combinatorial mapping rules given in Theorem 4.2 imply the Schottky relations, that a maps the interior of the A blob onto the exterior of the a blob and b maps the B blob onto the exterior of the b blob. Any pair of transformations that map a web of circles with this combinatorics must generate the $(5/8, -7/9)$ double cusp group, up to conjugacy.

There may be external tangencies that do not play a role in the definition of the Schottky curves. As an example, Figure 11 shows the $(\frac{3}{4}, \frac{1}{5})$ double cusp with the circle chains shaded darkly for $3/4$ and lightly for $1/5$. The orthogonal arcs are also drawn, and once again delineate four simple curves that obey the Schottky mapping conditions. One may see that there are two extra tangencies between dark and light disks not accounted for (nor precluded) by our theorem. The situation is more extreme when the pair of fractions $(\frac{p}{q}, \frac{r}{s})$ consists of Farey neighbors, because every such double cusp is conjugate to the Apollonian Gasket group. The complement of the corresponding web of circles consists only of disjoint ideal circular triangles.

5. Cusp groups on Riley's slice

In this section, we study the maximal cusps on the boundary of the deformation space of two-generator groups $\langle a, b\rangle$ where both a and b are parabolic and the quotient of

the ordinary set by the group is a four-times punctured sphere. These cusp groups are also maximal cusps on the boundary of the space of Schottky groups of genus two, but they are not in general cusps on quasifuchsian punctured torus space. This is called the *Riley slice* of Schottky space after Robert Riley who made the first detailed map of this space.

This is a one-complex-dimensional deformation space, and we shall use the parametrization

$$a = a_\rho = \begin{pmatrix} 1 & 0 \\ \rho & 1 \end{pmatrix} \qquad\qquad b = \begin{pmatrix} 1 & 2 \\ 0 & 1 \end{pmatrix} \tag{5.1}$$

of the associated groups $G_\rho = \langle a, b \rangle$ (we will recycle some notation from Section 2, since no use of that material will be made). When $|\rho|$ is sufficiently large, the ordinary set of this group is connected, and the quotient surface is a four-times punctured sphere. The domain of ρ for which this is true is topologically a punctured disk (with the puncture at ∞), with a cuspy roughly diamond-shaped inner boundary symmetrically arranged around the origin. An analysis of this boundary and the cusp groups is found in [KS98] (a revision of [KS94]).

The cusps on the boundary of Riley's slice are again associated to rational numbers p/q, $0/1 \le p/q \le 2/1$, with $\rho(2/1) = \rho(0/1)$. The rational number again describes the simple closed curve on the four-times punctured sphere that has been pinched to a point, as well as the word in the group G_ρ that has become accidentally parabolic. What we shall focus on here is how the rational number manifests itself in a web of circles in the limit set.

The following theorem is justified in [KS94].

Theorem 5.1. *Given a fraction $0/1 \le p/q < 2/1$, let $G_\rho = \langle a, b \rangle$ be the p/q cusp group on the boundary of Riley's slice. There are disjoint open disks δ_j, $0 \le j < 2q$, such that, we have*

$$a(\delta_j) = \delta_{2q-j} \quad \text{for } 0 \le j \le q; \qquad B(\delta_j) = \delta_{2p+2q-j} \quad \text{for } p \le j \le p+q,$$

where we define δ_j for all integers j by the periodicity condition $\delta_{j+2q} = \delta_j$. Moreover, the following pairs of disks are externally tangent:

- (δ_j, δ_{j+1}) *for* $0 \le j < 2q$*;*
- (δ_0, δ_q), (δ_p, δ_{p+q}).

With the normalization (5.1) *of G_ρ, the boundaries of δ_p and δ_{p+q} are horizontal lines (tangent at ∞), and δ_0 and δ_q are tangent at 0, the fixed point of a. The disks δ_j and δ_k are equivalent under G_ρ if and only if j, k have the same parity.*

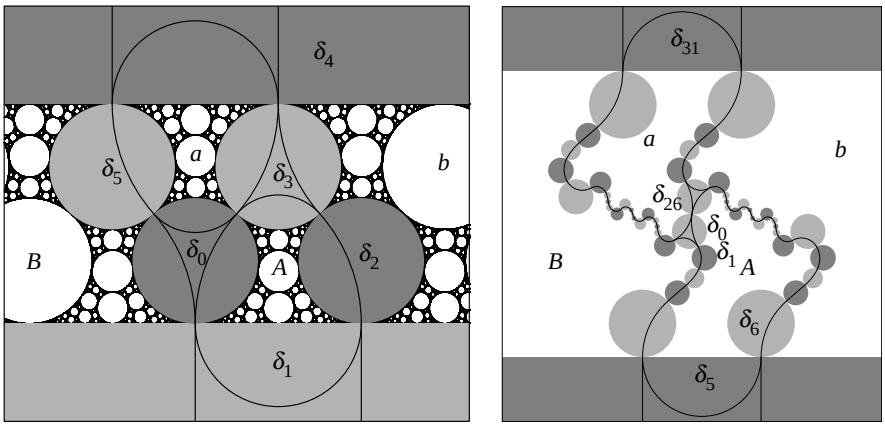

Figure 12: Chains of circles in cusp groups on Riley's slice. Left frame: the $\frac{1}{3}$ group; right frame: the $\frac{5}{26}$ group. The left includes the complete limit set in this frame.

Again, given such a circle web for a_ρ, b, we can conclude ρ is the p/q cusp on Riley's slice.

We illustrate this first in Figure 12 with the $1/3$ cusp group which, in our setup, turns out to have

$$\rho = -0.75 - 0.6614378278i.$$

The circles are labelled δ_0 through δ_5 in accordance with the theorem, with δ_6 being the same as δ_0. The shades of the disks indicate their equivalence class under the group; the picture shows clearly how the equivalence class alternates in order around the chain of circles.

As before, we have also connected all the tangent points in the chain with orthogonal arcs to the circles. These piece together into four Schottky blobs which are paired by a and b according to the Schottky mapping rules. For example, the tangent chain $\delta_0 \to \delta_1 \to \delta_2 \to \delta_3$ is mapped by a onto the chain $\delta_6 \to \delta_5 \to \delta_4 \to \delta_3$, and that implies that the interior of the A blob is mapped onto the exterior of the a blob. Again, the geometry of these external tangencies and Schottky curves immediately implies by Klein's combination theorem that the group is discontinuous and freely generated by a and b. With a little more work, this circle web identifies the group as the $1/3$ cusp group. The figure also shows all the visible part of the limit set of the group.

We have not revealed the recursive definition of the Riley p/q words comparable to the one given for Maskit p/q words in Section 2, but the dynamical definition can be read off the web of circles. The key is to keep track of a pair of tangent circles

under the mapping rules for a and b. As a shorthand notation, we use $i \wedge j$ to denote the pair of disks δ_i, δ_j, which are presumed to be one of the tangent pairs given in Theorem 5.1. Each pair of tangent disks lies on the boundary of precisely two of the four Schottky blobs. That means we can apply either of the transformations taking those blobs to the paired blobs and we will obtain another tangent pair of disks in the web of circles. That new pair will also lie on the boundary of precisely two blobs, and again there will be two possible transformations to apply. However, one will just lead back to the original pair of circles. Thus, if we continue to choose the new direction, we will gradually build up a word in the group that maps our original pair of circles to itself. By Lemma 2.2, that word is parabolic and stabilizes the tangent point of the pair of circles. That will be our Riley p/q word, up to conjugacy.

Let's begin this journey for the $1/3$ group starting with the pair $0 \wedge 1$ at the lower left in Figure 12. That lies on the boundaries of the A and B blobs, so that we can apply either a or b. We choose to begin with a; the other choice would simply lead to the inverse of the word we will eventually come up with. Our mapping rules are $a(j) = 6 - j$, for $0 \le j \le 3$, and $B(j) = 8 - j$, for $1 \le j \le 4$, with that for A and b being the inverse of these. Then going forward we obtain:

$$0 \wedge 1 \xrightarrow{a} 0 \wedge 5 \xrightarrow{b} 2 \wedge 3 \xrightarrow{a} 4 \wedge 3 \xrightarrow{B} 4 \wedge 5 \xrightarrow{A} 2 \wedge 1 \xrightarrow{B} 0 \wedge 1$$

Reading from right to left, the word that stabilizes $0 \wedge 1$ is *BABaba*, which can be taken to be the $1/3$ Riley word. The stabilizers of all the tangent pairs other than $0 \wedge 3$ (fixed by a) and $1 \wedge 4$ are cyclic permutations of this word. In particular, the stabilizer of $1 \wedge 2$ is $b(BABaba)B = ABabaB$. The fuchsian subgroup of $\langle a, b\rangle$ that stabilizes the lower half-plane δ_1 is the group generated by b and *BABaba*, or alternatively by B and *ABaba*. Since $\operatorname{tr} ABaba = \operatorname{tr} a = 2$, as they are conjugate, and we have set $\operatorname{tr} b = 2$, we conclude the cusp group occurs at a solution ρ to $\operatorname{tr} BABaba = -2$. The reason is that a triply-punctured sphere group $\langle u, v\rangle$ with u, v and uv parabolic can never have a representation in which $\operatorname{tr} u = \operatorname{tr} v = \operatorname{tr} uv = 2$. Note that the fractions $0/1$ and $1/1$ are somewhat special cases, as the groups are fuchsian (*the* triply-punctured sphere group), and the above procedure has to be suitably interpreted to produce the correct words. The second picture in Figure 12 shows the more complicated $5/26$ cusp group.

6. Maximal cusps in the Schottky space of genus g

In this final section, we wish to cull the common themes running through our previous examples into a model of the geometry of maximal cusps on the boundary of Schottky space of genus g. In particular, we will define the *circle web* of a maximal cusp and describe some of its basic properties. Let G be a discrete group freely generated by the

Möbius transformations $a_1, \ldots, a_g$. We shall assume that G is a maximally parabolic group. By Theorem II of [KMS93], G is geometrically finite. By this and Theorem 2 in [Mas81], we know that G is an accessible point on the boundary of the Schottky space of genus g, meaning that G is an algebraic limit of Schottky groups. By Theorem I of [KMS93], every component of the ordinary set of G is a circular disk, on which G represents a triply-punctured sphere. The circle web is a finite selection of these disks determined by the nature of the limit points on their bounding circles.

The infinite words in the generators $a_1^{\pm 1}, \ldots, a_g^{\pm 1}$ are the usual infinite sequences of choices from the generators or their inverses, satisfying the rule that no two consecutive terms are inverse to each other. The space of infinite words is endowed with the dictionary topology. This space is also known as the *completion* (or *boundary*) $\overline{G}$ of the group G relative to the given generator set. This notion was introduced in [Flo80], where it was proved that there is a continuous mapping from $\overline{G}$ to the limit set $\Lambda(G)$ of G. In this case, the mapping is defined by sending the infinite word $w = u_1 u_2 u_3 \cdots$ to the limit point $\phi(w) = \lim_{n\to\infty} u_1 u_2 \cdots u_n(z)$ for almost any seed point z. Floyd also proved that the mapping ϕ is injective everywhere except at the inverse images of fixed points of parabolic elements of G, where it is two-to-one. If z is the fixed point of a parabolic word p with inverse P, then $\phi^{-1}(z)$ consists of the two infinite words $pppp\cdots$ and $PPPP\cdots$, allowing for some cancellation.

With this notation, we may now divide the limit set $\Lambda(G)$ into subsets defined by

$$\Lambda(a) = \{z \in \Lambda \mid z = \phi(aw) \text{for some infinite word } aw \text{ beginning with } a\}$$

for any choice of a from $\{a_1^{\pm 1}, \ldots, a_g^{\pm 1}\}$. We now define the *circle web* as the circles that separate these subsets of $\Lambda(G)$.

Definition 6.1. For a maximal cusp group G on the boundary of Schottky space, we define the *circle web of G*, relative to the designated generators $a_j^{\pm 1}$, to consist of each circular disk in the ordinary set of G whose boundary circle contains points from at least two different subsets $\Lambda(a)$, $a \in \{a_1^{\pm 1}, \ldots, a_g^{\pm 1}\}$.

In the topology of the space of infinite words, the subset of those words beginning with a fixed prefix is closed. Since the mapping ϕ is continuous by Floyd's theorem, each of the subsets $\Lambda(a)$ is closed as well.

In [Mas83], Maskit gave a general description of the collections of words that may become parabolic in a deformation of a function group. In the case of a maximal cusp group on the boundary of Schottky space of genus g, all parabolic words are conjugate to a power of one of a list of $3g-3$ words corresponding to a maximal system of isotopy classes of disjoint simple closed curves on a surface of genus g,

or alternatively a pair-of-pants decomposition of this surface. Each parabolic word is doubly cusped (see [Mas81]), meaning that it fixes precisely two disks in the ordinary set, which are externally tangent at the fixed point of the word.

In the free group, a word u of minimum length in any conjugacy class must be such that u and its inverse U begin with different choices from the generators $a_j^{\pm 1}$, $1 \leq j \leq g$. Otherwise, u would be of the form avA, and thus conjugate to a shorter word v. If u has length n which is minimal in the conjugacy class of u, there are at most n elements of length n in the class of u, namely, all the cyclic permutations of u. Furthermore, if u is not a power of another element, then all the cyclic permutations of u are distinct words. The fixed points of a cyclic permutation w of u correspond to two distinct infinite words $www\cdots$ and $WWW\cdots$, which begin with different generator letters, and thus belong to two different subsets $\Lambda(a)$. Since the mapping from infinite words to limit points is at most 2-to-1, this also implies the fixed points of distinct cyclic permutations of u are different, given that u is not a power.

Each of these fixed points of minimal length parabolic words is a tangent point between two circles in the circle web. If w_j, $1 \leq j \leq 3g-3$, is a maximal list of non-conjugate and non-inverse minimal length parabolic words in the maximal cusp group G, the number of these tangent points is precisely $\sum_j |w_j|$, where $|w|$ denotes the length of the word w. Each circle in the circle web must contain at least two of these fixed points, dividing the circle into arcs each belonging entirely to one of the subsets $\Lambda(a)$ of the limit set. These observations prove the following.

Proposition 6.2. *There are only finitely many disks in the circle web of a maximal cusp group. To be precise, let w_j, $1 \leq j \leq 3g-3$, be a maximal list of minimal length parabolic words which are non-conjugate and non-inverse. The fixed points of all the cyclic permutations of these words are tangent points between pairs of disks in the circle web. The number of tangent points is thus the sum of the lengths of this list of parabolic words, and the number of circles is at most this same sum.*

Each circle in the web contains at least two of these tangent points. Connect the consecutive tangent points going around the circle by arcs which are interior to the circle and orthogonal to it. We will call these the *orthogonal arcs* to the circle web. Label an orthogonal arc with generator a if there is an arc of the boundary circle connecting the endpoints of the orthogonal arc and belonging entirely to the subset $\Lambda(a)$ of the limit set. Each orthogonal arc will then have one or two generator labels. If it has two labels, the corresponding circle in the web contains only that one orthogonal arc. The orthogonal arcs, without the labels, are all drawn in Figures 2, 2, 11, 12.

Consider the orthogonal arcs meeting a given tangent point between two circles in the web. The tangent point is the fixed point of a parabolic word beginning with generator a and ending with generator B, and a and B are non-inverse. Thus, the orthogonal

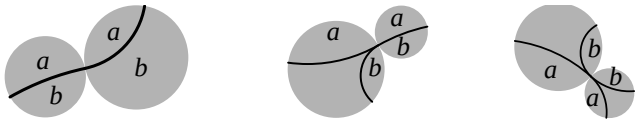

Figure 13: Possible meetings of the orthogonal arcs at a tangent point between two circles in the web.

arcs ending at that point are labelled a or b or both. Then, in each circle, there are one or two orthogonal arcs ending at that tangent point. The three possibilities for these arcs and their labels are shown in Figure 13.

For a particular generator a, now consider only the collection of orthogonal arcs labelled with a. By the previous paragraph, these arcs form a combinatorial graph in which each vertex has degree 2. Thus, this graph is a disjoint union of loops. We would like to prove there is exactly one loop. There must be at least one since some of the list of parabolic words must include a as a term, for otherwise we could further deform the group to one in which a is also parabolic, contrary to our assumption of maximality. (Since the list of parabolic words does not include a as a term, we are free to define a to be a parabolic transformation that identifies two very small tangent circles inside a fundamental region for the group generated by the other generators.)

To prove there is only one a loop, we need a more precise description of the list of parabolic words $w_1, \dots w_{3g-3}$. We consider the corresponding simple closed curves $\omega_1, \dots, \omega_{3g-3}$ on the associated surface of genus g. At the same time, there are disjoint simple closed curves γ_j on the surface corresponding to the generators a_j, $1 \le j \le g$. These are the curves coming from the pair of loops in the plane that are paired by the generators of the Schottky group. We shall assume that all the curves are arranged to have minimal intersections. An example of a maximal system of six disjoint curves is sketched in Figure 14.

The word associated to each simple closed curve ω_i may be discovered by following the curve through its intersection points with each of the generator curves γ_j. Label one side of γ_j by the generator a_j and the other side by the inverse a_j^{-1} according to the loops in the plane that are paired by a_j. Starting at one intersection point of the curve ω_i, we pick one direction and follow the curve to the next intersection point in that direction. If the curve passes from the a_j^{-1} to the a_j side at that intersection point, we write down the letter a_j; otherwise, we write down a_j^{-1}. Continuing to the next intersection point in that direction, we make the analogous observation and write the next generator to the left of the previous way. In this way, when we return to our starting point we will have written down the word corresponding to this curve with the

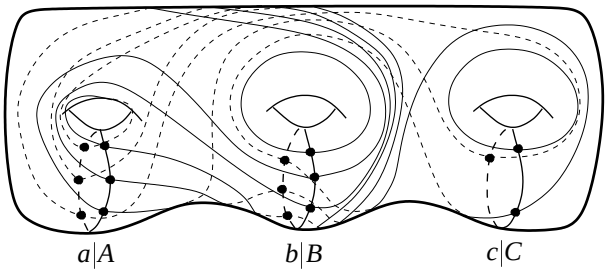

Figure 14: A system of six disjoint loops on a surface of genus 3. The generator curves are labelled by the respective generator *a*, *b* and *c*. The curves correspond to the words *b*, *c*, *bC*, *acAB*, *baa* and *abAB*. Dotted lines signify parts of the curve on the back side of the surface.

given starting point and given direction.

This associates to each intersection point two words, one for each direction. The collection of words obtained in this way are all the cyclic permutations of the original list $w_1, \ldots, w_{3g-3}$ and their inverses. The words associated to the intersection points lying on the generator curve γ_j are all those words beginning with a_j and all those beginning with a_j^{-1} (in the reverse direction). As we follow the curve γ_j around its handle, adjacent intersection points either belong to the same curve ω_i or they belong to two distinct curves that bound the same pairs of pants.

If the two words u_1 and u_2 (both beginning with a_j) for those adjacent intersection points bound the same pair of pants, then there is a third word u_3 corresponding to the third bounding curve of the pair of pants such that u_3 is conjugate to $u_1^{-1}u_2$. It follows then that in the maximal cusp group G, when all three words are parabolic, the words u_1 and u_2 generate a triply punctured sphere group (since $u_1^{-1}u_2$ is also parabolic) corresponding to one of the circular disks in the ordinary set of G. Since u_1 and u_2 both begin with a_j and do not end with a_j^{-1}, it follows that they are connected by an orthogonal arc labelled a_j.

If the adjacent intersection points actually lie on the same curve ω_i and the curve passes through γ_j in the same direction at the two points, then this curve forms two boundary components of a pair of pants. The third boundary component again corresponds to a conjugate of $u_1^{-1}u_2$. The same argument as before again proves that u_1 and u_2 generate a triply-punctured sphere group in the maximal cusp, and that the fixed points of u_1 and u_2 are connected by an orthogonal arc.

Finally, if the same curve passes through adjacent points on γ_j in opposite directions, then u_1 and u_2^{-1} are conjugate words, and the conjugating word u_3 corresponds to one of the other two boundary components of the pair of pants bounded by our original curve. That is, $u_2^{-1} = u_3 u_1 u_3^{-1}$. In the maximal cusp group u_1, u_2 and u_3 are

all parabolic, implying the again that the fixed points of u_1 and u_2 are connected by an orthogonal arc in the circle web.

Thus, the orthogonal arcs labelled with a_j pass through in order the fixed points of the words corresponding to the intersection points lying on γ_j, which are all the words beginning with a_j. This proves there is exactly one loop of orthogonal arcs labelled a_j. We summarize our work as follows.

Theorem 6.3. *Let $G = \langle a_1, \ldots, a_g \rangle$ be a maximal cusp group. Let $w_1, \ldots, w_{3g-3}$ be the complete list of minimal length parabolic words which are non-conjugate and non-inverse. Label each disk δ in the circle web of G with each generator a among the $a_j^{\pm 1}$'s for which δ has nonempty intersection with $\Lambda(a)$. The following are true.*

(i) *The disks labelled a form a loop of disjoint disks $\delta_1, \ldots \delta_n$ in which each δ_i is tangent to δ_{i+1}, and δ_n is tangent to δ_1. The number n of these disks equals the number of a's and a^{-1}'s occurring in the expressions of the minimal length parabolic words w_k in terms of the generators of G. Call this loop the a loop of circles. The a and a^{-1} loops contain the same number of circles.*

(ii) *The orthogonal arcs labelled a form a simple closed loop passing through the tangent points of the a loop of circles. The subset $\Lambda(a)$ of the limit set consists precisely of all the limit points contained in one component of the complement of this simple closed curve.*

(iii) *The generator a maps the a^{-1} loop of circles onto the a loop of circles in reverse order relative to the subsets $\Lambda(a^{\pm 1})$ they enclose.*

The circle web can be described by a combinatorial graph where the vertices are the disks and the edges correspond to pairs of disks which are tangent at fixed points of minimal length parabolic words. (The right side of Figure 11 shows there may be other tangent points, not corresponding to edges.) The previous theorem shows that this is a planar graph with $2g$ faces labelled by each of the generators and their inverses. The degrees of paired faces, meaning the number of vertices around each face, are equal.

On the other hand, by taking a planar graph with $2g$ paired faces, with paired faces of equal degree, we may choose mappings of the vertices around the a_j^{-1} face onto those around the a_j face in reverse order. Then by following these mappings around the graph we may calculate the word stabilizing each vertex. This process was described at the end of Section 5 for a Riley group. If we end up with a collection of $3g-3$ words corresponding to a maximal system of simple closed curves on a surface of genus g, we may solve the polynomial equations derived from setting the traces of these words equal to ± 2 to find matrices that generate a corresponding maximal cusp.

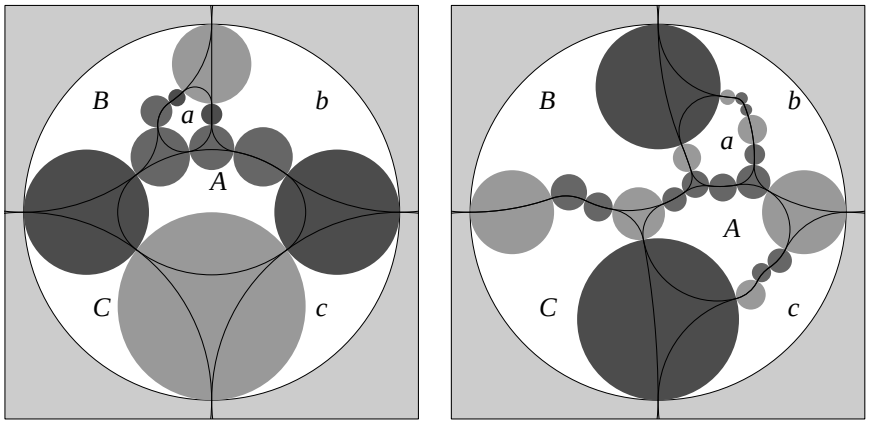

Figure 15: Circle webs for maximal cusps on the Schottky space of genus 3. The orthogonal arcs connecting the tangent points again piece together to form Schottky "blobs." The paired blobs are marked $a \leftrightarrow A$, $b \leftrightarrow B$, $c \leftrightarrow C$, in such a way that a takes the interior of the A blob onto the exterior of the a blob, etc. The shade of the disk indicates its equivalence class. The collection of minimal length parabolic words for the righthand picture is $\{b, c, bC, acAB, BacBAbCAba, BacBaaa\}$.

In this way, in a future work we hope to calculate a catalog of many cusps and some idea of the geometry of the boundary of Schottky space.

Two precise examples are shown in Figure 15. The left corresponds to the system of curves sketched in Figure 14. The second comes from a more complicated system of curves.

References

[BDS94] Alan F. Beardon, Tomasz Dubejko, and Kenneth Stephenson, *Spiral hexagonal circle packings in the plane*, Geom. Dedicata **49** (1994), 39–70.

[Ber70] Lipman Bers, *On boundaries of Teichmüller spaces and on kleinian groups, I*, Ann. of Math. (2) **91** (1970), 570–600.

[Bro85] Robert Brooks, *On the deformation theory of classical Schottky groups*, Duke Math. J. **52** (1985), no. 4, 1009–1024.

[CCHS03] R. D. Canary, M. Culler, S. Hersonsky, and P. B. Shalen, *Approximation by maximal cusps on the boundary of quasiconformal deformation space*, J. Differential Geom. **64** (2003), 57–109.

[Flo80] William J. Floyd, *Group completions and limit sets of kleinian groups*, Invent. Math. **57** (1980), 205–218.

[KMS93] Linda Keen, Bernard Maskit, and Caroline Series, *Geometric finiteness and uniqueness for Kleinian groups with circle packing limit sets*, J. Reine Angew. Math. **436** (1993), 209–219.

[KS92] Linda Keen and Caroline Series, *Pleating coordinates for the Teichmüller space of a punctured torus*, Bull. Amer. Math. Soc. (N.S.) **26** (1992), 141–146.

[KS93] ———, *Pleating coordinates for the Maskit embedding of the Teichmüller space of punctured tori*, Topology **32** (1993), 719–749.

[KS94] ———, *The Riley slice of Schottky space*, Proc. London Math. Soc. (3) **69** (1994), 72–90.

[KS98] Yohei Komori and Caroline Series, *The Riley slice revisited*, The Epstein birthday schrift, Geom. Topol. Monogr., vol. 1, Geom. Topol. Publ., Coventry, 1998, pp. 303–316 (electronic).

[KS04] Yohei Komori and Toshiyuki Sugawa, *Bers embedding of the Teichmüller space of a once-punctured torus*, Conform. Geom. Dyn. **8** (2004), 115–142.

[KSWY] Y. Komori, T. Sugawa, M. Wada, and Y. Yamashita, *Drawing Bers embeddings of the Teichmüller space of once-punctured tori*, to appear.

[KT90] S. P. Kerckhoff and W. P. Thurston, *Non-continuity of the action of the mapping class group at Bers' boundary of Teichmüller space*, Invent. Math. **100** (1990), 25–47.

[Mas74] Bernard Maskit, *Moduli of marked Riemann surfaces*, Bull. Amer. Math. Soc. (N.S.) **80** (1974), 773–777.

[Mas81] ———, *On free Kleinian groups*, Duke Math. J. **48** (1981), 755–765.

[Mas83] ———, *Parabolic elements in Kleinian groups*, Ann. of Math. (2) **117** (1983), 659–668.

[McM91] C. McMullen, *Cusps are dense*, Ann. of Math. (2) **133** (1991), 217–247.

[Min99] Yair N. Minsky, *The classification of punctured-torus groups*, Ann. of Math. (2) **149** (1999), no. 2, 559–626.

[Miy02] Hideki Miyachi, *On the horocyclic coordinate for the Teichmüller space of once punctured tori*, Proc. Amer. Math. Soc. **130** (2002), no. 4, 1019–1029 (electronic).

[Miy03] ———, *Cusps in complex boundaries of one-dimensional Teichmüller space*, Conform. Geom. Dyn. **7** (2003), 103–151 (electronic).

[MSW02] David Mumford, Caroline Series, and David Wright, *Indra's Pearls: The Vision of Felix Klein*, Cambridge University Press, 2002.

[Par95] Jouni Parkkonen, *Geometric complex analytic coordinates for deformation spaces of Koebe groups*, Ann. Acad. Sci. Fenn. Ser. A I Math. Dissertationes (1995), no. 102, iv+50.

[Sch97] Oded Schramm, *Circle patterns with the combinatorics of the square grid*, Duke Math. J. **86** (1997), no. 2, 347–389.

[Sco] Irene Scorza, *The core chain of circles in Maskit's embedding for once-punctured torus groups*, preprint.

[Ste] Kenneth Stephenson, *Introduction to circle packing and the theory of discrete analytic functions*, Cambridge University Press, to appear in 2005.

[Thu80] W. Thurston, *The geometry and topology of 3-manifolds*, Princeton University Press, Princeton, 1980.

[Thu82] ———, *Three-dimensional manifolds, kleinian groups, and hyperbolic geometry*, Bull. Amer. Math. Soc. (N.S.) **6** (1982), 357–382.

[Thu89] ———, *Groups, tilings, and finite state automata*, Tech. Report GCG1, Geometry Supercomputer Project Research Report, 1989, Summer 1989 AMS Colloquium Lectures.

[Wri87] David J. Wright, *The shape of the boundary of the Teichmüller space of once-punctured tori in Maskit's embedding*, preprint, 1987.

David J. Wright

Department of Mathematics
Stillwater, OK 74078 wrightd@math.okstate.edu

kleinian@maths.warwick.ac.uk

AMS Classification: 30F40, 22E40, 57S30

Keywords: Kleinian groups